Structural Evaluation and Preliminary Analysis of the St. Jerome Hall of the Church of the Nativity in Bethlehem

E. Mauricio Gonzales[1], Miguel A. Pando[2], Matthew Whelan[2], Dante Fratta[3], Luis F. Ramos[4], and Rafael Aguilar[1(✉)]

[1] Civil Engineering, Pontificia Universidad Católica del Perú PUCP, Lima, Peru
{emgonzales, raguilar}@pucp.pe
[2] Civil and Environmental Engineering,
University of North Carolina at Charlotte, Charlotte, USA
{mpando, m.whelan}@uncc.edu
[3] Geological Engineering, University of Wisconsin-Madison, Guimarães, USA
fratta@wisc.edu
[4] Civil Engineering, Universidade do Minho, Guimarães, Portugal
lramos@civil.uminho.pt

Abstract. The St. Jerome Hall (SJH) located within the Church of the Nativity complex in Bethlehem, Palestine, is a stone masonry building originally built circa the 4th Century. Excavations associated to an archaeological project inside the SJH has exposed structural and foundation elements creating concerns of potentially inadequate structural and foundation performance. This paper summarizes the results of an in-situ study aimed at assessing the structural and foundation condition considering the archaeological-related excavations. The structural assessment involved a detailed laser scanning survey, visual inspections, IR thermography and a wide variety of nondestructive testing (surface wave analysis and operational modal analysis). Nondestructive testing (NDT) allowed for the evaluation of mechanical responses of different structural elements as well as identification of damage. A 3D finite element (FE) model was then used to evaluate the current level of loading at the base of the columns and walls, as well as at the ceiling influenced by the current excavated condition of the hall. Numerical results showed that the current stresses in walls and columns are lower that the estimated strength; however, retrofitting should be considered in one of the columns to avoid compromising the stability of the structural system.

Keywords: Masonry structure · In situ testing · Damage analysis
Historical building · Numerical modelling

1 Introduction

The Church of the Nativity in Bethlehem is an important cultural and religious monument that was declared a UNESCO World Heritage Site on 2010. According to the Palestinian Central Bureau of Statistics, more than 400 thousand pilgrims and tourists

annually visit Bethlehem and its church [1]. The church hosts the grotto that is believed to be the location of the birth of Jesus. Religious tourism is one of the main economic activities of the region, producing more than US$ 600 million and employing around 20% of the local population in 2014 [1]. Figure 1a shows a plan view of the western part of the church complex, the Armenian monastery, and the location of the St. Jerome Hall (SJH).
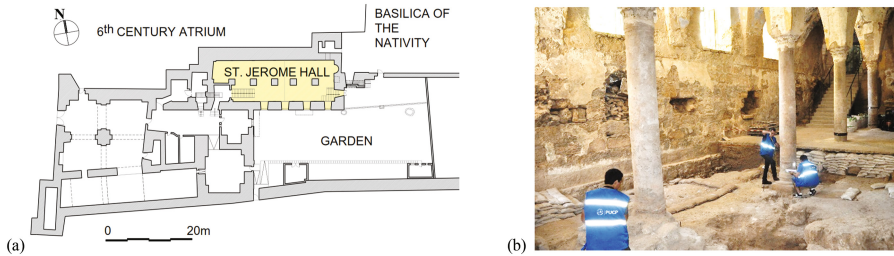

Fig. 1. (a) Plan view of the Armenian monastery and (b) photograph from the East showing the excavated area inside the SJH [3].

Construction of this building began in the 4th Century by order of emperor Constantine the Great, followed by major modifications during the 6th Century [2]. The last global modification included the construction of the SJH during the Crusades, between the 11th and 12th Centuries [2]. The SJH is a 9.1 m by 26.2 m rectangular room. Structurally, the room has massive masonry walls along the N and S sides. The ceiling of the hall is formed by arches supported by walls along the perimeter of the room and by four stone columns and one masonry column that are located along the E to W centerline axis (Fig. 2b). The southern wall of the SJH is a massive masonry wall approximately 1.9 m thick that is partially buried along its southern face. The northern wall is also a masonry wall with an average overall thickness of 2.75 m. This northern wall increases in width along the eastern side due to the presence of a small room that connects it to the Basilica of the Nativity. The northern wall is also partially buried along its northern face, which is exposed to the 6th Century Atrium.
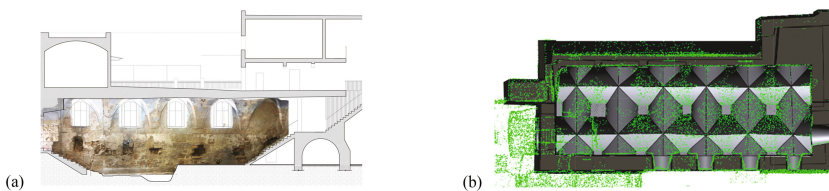

Fig. 2. Geometrical survey of the SJH: (a) southern wall elevation, and (b) solid blocks (adapted from [3])

This paper documents part of a study requested by the archaeologist on behalf of the Armenian Patriarchate to assess the structure and the stability of walls and columns of the SJH. To assess the stability of the structure, a multidisciplinary team comprised of experts in the field of structural diagnosis, foundation engineering, nondestructive testing, and health monitoring was assembled to conduct the field study during a week in July 2016. As part of this structural diagnosis study, the geometry of the SJH was profiled using 3D geometrical surveying and reconstruction techniques. Then, structural assessment of material properties was performed through nondestructive testing, including Sonic Indirect Test (SIT) and Impact Echo Test (IET). The dynamic properties of the structure were also measured using operational modal analysis (OMA) to assist in the structural assessment. Using the measured material properties and modal parameters, a 3D Finite Element Model (FEM) was developed to estimate current level of loading of the walls and columns and potential redistribution of stresses within SJH resulting from the recent excavations in the hall.

2 Geometrical Survey and 3D Reconstruction

The Church of the Nativity complex has a complicated construction history that is not well documented. Consequently, a geometrical survey was performed to develop dimensioned plans and a 3D model of the study area. Both Terrestrial Photogrammetry (TP) and Terrestrial Laser Scanning (TLS) were applied to develop 3D reconstruction of the SJH. The 3D TP reconstruction was performed using a texturized 3D model and orthophotographs of the interior of the SJH. A 23 MPixel camera was used to acquire 93 photographs, which were processed to develop a 3D rendering of the complex using AgisoftPhotoScan software [4]. In addition to the TP reconstruction, the detailed geometry of the SJH and the connected structures was acquired using a total of 28 scanning sessions with a Leica MS50 Multi-Station laser scanner. The data processing involved the registration and denoising of the point cloud. The 3D renderings developed by each technique were used as a basis for the generation of plans and the geometry for the FEM. Figure 2a shows an orthophotograph of the inside elevation of the southern wall. While, Fig. 2b presents part of the refined point cloud profiling of the complex geometry of the ceiling of SJH, which was later exported to assist in the creation of the FEM.

3 Structural and Foundation Assessment

The structural and foundation assessment began with a detailed visual inspection of the SJH to identify and document any evidence of structural damage. Then, nondestructive testing (NDT) in the form of indirect and impact echo sonic tests and operational modal analysis (OMA) through ambient vibration monitoring were performed to characterize mechanical properties and inform performance-based condition assessment.

3.1   Damage Visual Inspection

The main structural pathologies were identified through visual inspection and infrared thermography. Figure 3a summarizes the location of the observed pathologies inside the SJH. As shown in this figure, two potential structural problems were identified. The first structural anomaly was related to the exposed condition of the foundation of the eastern column (Column C1) (Fig. 3b). Also a small crack was visible at the base of the column that appeared to cross the plinth and extend into the underlying foundation layer. The second structural anomaly is associated to the existence of 2-mm wide cracks in the capitol of Column C4. Other observed damages included plaster deterioration and moisture in the walls and the ceiling of the SJH.
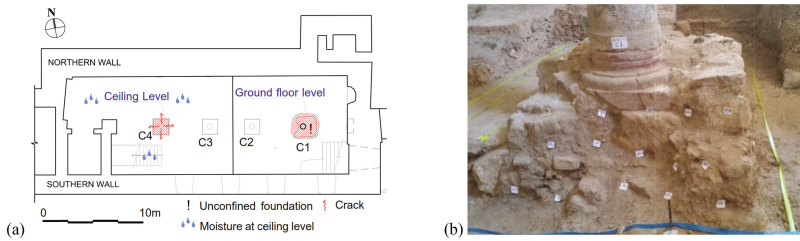

Fig. 3. Damage assessment of the SJH: (a) location of the main pathologies, and (b) exposed foundation of Column C1 [4].

3.2   Nondestructive Testing and Material Properties Assessment

SIT and IET were used to nondestructively estimate the mechanical properties of the four stone columns of the SJH and the masonry in the northern and southern walls. The locations of each test, both inside and outside the hall are shown in Fig. 4a. Figure 4b and c show digital photographs of the impact echo and indirect sonic tests, respectively, being performed in the field.
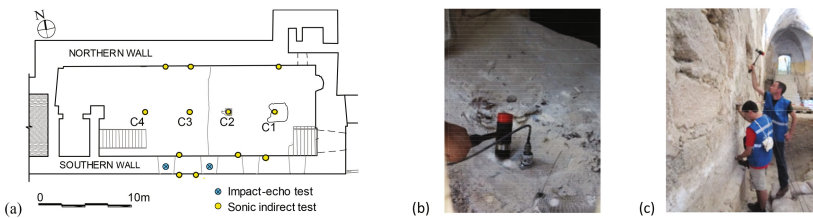

Fig. 4. Nondestructive test in the SJH: (a) location of the test, (b) impact echo test and (c) indirect sonic test [3].

Knowing the ratio between the Raleigh wave velocity and the P-wave velocity (V_R/V_P) and the mass density, it is possible to estimate the Poisson's ratio (v) and the Young's modulus (E) [5] of the tested elements. In the following analysis, the mass

density of masonry and of columns was assumed to be between 1800–2200 kg/m^3 and 2400–2600 kg/m^3 [6], respectively. The static E of masonry was considered to be equal to 80% of the dynamic E obtained through SIT, while the static E of stone columns were considered to be 90% of the values obtained through SIT [7]. The estimated values, shown in Table 1 are plausible for this type of structure [5].

Table 1. Summary of sonic testing results [3] and estimated material properties.

Property	North Wall		South Wall		Stone Columns	
	Average	Covariance (%)	Average	Covariance (%)	Average	Covariance (%)
V_R/V_P	0.53	5	0.62	1	0.59	0.59
Poisson's ratio ν	0.24	21	0.19	2	0.20	–
Minimum static E [GPa]	1.74	53	4.40	25	78.2	16
Maximum static E [GPa]	2.12	53	5.38	25	84.6	16

IET was performed on the bottom surface of the two windows of the southern wall, to estimate the foundation depth of the masonry wall. The results for both impacts gave, on average, reflections at depths of 1.4 m, 4.5 m and, 8.7 m with a confidence of ±0.96 m. The reflection at 4.5 m was determined to be the depth of the south wall due to being relatively coincident with the level of the archeological excavation.

3.3   Operation Modal Analysis (OMA)

To complement the other components of the structural assessment of the SJH, ambient vibration measurements were made at various locations within the structure. OMA was performed to identify the modal parameters of the structure, including the natural frequencies, mode shapes, and damping coefficients. The ambient vibration monitoring consisted of the measurement of accelerations at 17 degrees of freedom. The configuration of measurement axes is shown in Fig. 5a, where it is denoted that nine axes were located at the second floor elevation and the remaining eight were located at the roof elevation. The transducers used in the study were piezoelectric accelerometers with a sensitivity of 1000 mV/g and a full-scale measurement range of ±0.5 g. The accelerometers were bolted to aluminum positioning blocks and adhered to the structure using a temporary adhesive (Fig. 5b). A 24-bit data acquisition system was used to simultaneously sample the transducers at a sampling rate of 256 Hz (Fig. 5c). Reference-based ambient vibration monitoring was performed using three configurations with three stationary reference accelerometers to produce coverage of the 17 measurement axes. The sampling duration for each tests was 13 min.

OMA was carried out using the Stochastic Subspace Identification (SSI) technique [8]. SSI allowed for the identification of the 4 first natural frequencies, mode shapes, and

Fig. 5. OMA test: configuration scheme, (b) piezoelectric accelerometer, and (c) acquisition system.

damping coefficients. Figures 6a, b, and c present the experimental estimates for the fundamental modes in the North, East, and torsional directions, respectively. Figure 6d presents the experimental estimate for the fourth mode shape, which features a combined response of torsion and flexure. The results of OMA are useful for assessing the structural condition, since they help to measure the numerical model correlation with the experimental modal parameters.
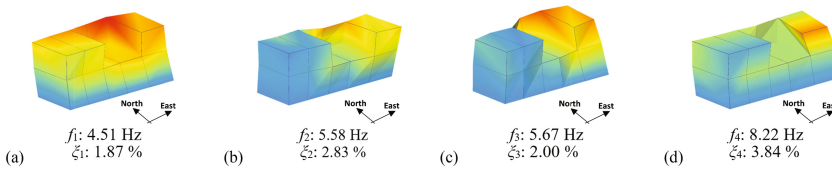

(a) f_1: 4.51 Hz ξ_1: 1.87 % (b) f_2: 5.58 Hz ξ_2: 2.83 % (c) f_3: 5.67 Hz ξ_3: 2.00 % (d) f_4: 8.22 Hz ξ_4: 3.84 %

Fig. 6. OMA test results: modal shapes, frequencies (f) and damping coefficients (ξ).

4   Numerical Modelling

A FEM was developed to assist with the structural assessment of the SJH. The development of the FEM included the import of the geometries from the geometrical surveys, the election of element types, the definition of the boundary conditions, and the generation of the FE mesh. The model provides for representation of the main components that compose the SJH: columns, capitols; and limestone masonry. Each of these components were modeled with solid elements with their respective material properties (Fig. 7a). Initial elastic properties were obtained from SIT. The model presented in this paper was developed as a preliminary tool to provide a preliminary assessment of the structural condition; where, tetrahedral elements with 4 nodes and 3 sides were used [9]. These types of elements can better fit the geometry of the vaulted ceiling. Soil-structure interaction for the embedded portions of the walls was accounted for in a simplistic manner through the use of equivalent linear elastic springs with a constant stiffness (K) along depth, and oriented normal to the surface of each wall. Figure 7 shows the FE mesh and the representation of boundary conditions with elastic springs.
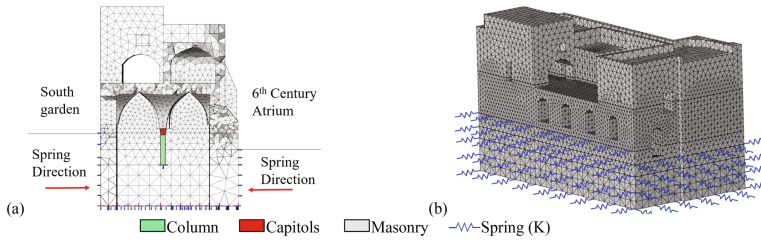
Fig. 7. FE mesh implementation: (a) materials, boundary conditions, and (b) location of springs.

4.1   Calibration of the FEM Using OMA Results

The calibration process was carried out through a parametric analysis in which the static E of masonry and the spring constant (K) were varied systematically to minimize the difference between the natural frequencies and mode shapes computed by the FEM and those experimentally obtained through the OMA. The Modal Assurance Criterion (MAC) and Modal Assurance with Frequency Scales (FMAC) were additional statistical indicators used for this analysis [10]. Table 2 shows the range, the interval precision, and final estimated value of the static E and K that resulted in the best correlation with the experimental modal parameter estimates from the OMA. The influence of static E on the relative frequency prediction, and K on the MAC is shown in Fig. 8a and b, respectively. Note that as static E of masonry increases, the frequency error exceeds a reasonable limit. In order to optimize the MAC and to reduce the frequency error, the Douglas Reid's approach [11] was used. Figure 8c shows the final FMAC graphic where all MAC values are greater than 0.75 and the maximum error in natural frequency is less than 10%. It should be noted that the final value for static E (1.50 GPa) is smaller than static E estimated through the SIT performed in the northern wall (1.74 to 2.12 GPa) and substantially smaller than estimated on the southern wall (4.40 to 5.38 GPa). This result suggests that, despite the calibration of the FEM, there are likely significant errors in the modeling assumptions that remain uncorrected.

Table 2.   Mechanical parameters varied for the calibration process.

Property	Minimum	Interval	Maximum	Final
Masonry - static modulus E [GPa]	1.20	0.10	2.0	1.50
Soil - spring constant K [kN/m]	0	1000	23000	20000

4.2   Preliminary Structural Static Analysis

Using the calibrated FEM of the SJH, a preliminary static analysis of SJH was performed. The structural analysis involved the investigation of the current level of loading of the walls and columns. The total strain crack model was used as the constitutive model for masonry [9, 12]; while columns and capitols were assumed to remain linearly elastic. Using indirect correlations [13, 14], it was possible to estimate the mechanical properties of masonry, namely compressive strength f_c, tensile strength
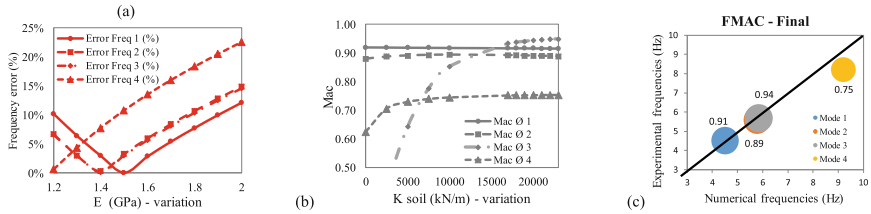
Fig. 8. Influence of (a) static modulus E on frequency relative error, (b) spring constant K on mode shapes, and (c) final FMAC.

f_t and their respective fracture energies G_c and G_t. Table 3 summarizes the mechanical properties assigned to the three main components. The static loads considered in the analysis were gravity, loads related to standard usage (estimated as 2500 Pa), and possible snow load (1400 Pa) for the winter conditions. The FEM included the lateral earth pressures, and also the load due to the water tanks located at the roof. Figure 9a presents the computed deviatoric strains, and shows that the maximum strain is around $1.45 \cdot 10^{-3}$ located over the capitol of Column C4 due to the significant mass above its element. Figure 9b presents the compressive stresses at the bottom of the perimeter walls of SJH. These stresses ranged from 0.194 to 0.426 MPa and were found to be greater in the western side of the southern wall since this section supports a heavier load in the second floor due to offices. This compressive stress level is around 22% of the estimated wall compressive strength that was appraised from the indirect sonic tests results.

Table 3. Mechanical properties considered for the structural analysis.

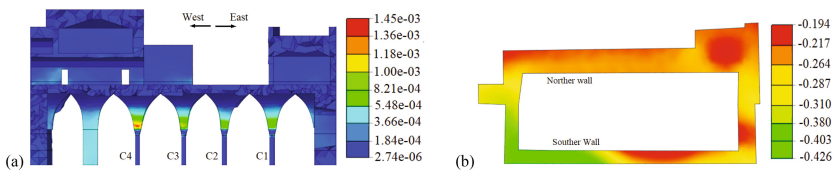| Property	E [GPa]	Poisson's ratio	Density [kg/m^3]	f_c [MPa]	G_c [kN/m]	f_t [MPa]	G_t [kN/m]
Masonry	1.50	0.20	2000	3.54	5690	0.15	0.15
Capitols	35	0.20	2200	Elastic	Elastic	Elastic	Elastic
Columns	70	0.20	2500	Elastic	Elastic	Elastic	Elastic

Fig. 9. Numerical results: (a) deviatoric strains [mm/mm] and (b) level of stress in walls [MPa]

The FE model results indicates compressive stress levels at the base of columns C1, C2, C3 and C4 of 5.69, 3.85, 8.08, and 8.76 MPa; respectively. These estimated stress levels correlate well with the observed variation in the mass above each column.

In addition, compressive stress levels at each column are significantly lower than the compressive strength of Judean limestone, which typically varies between 64 to 187 MPa [15].

5   Summary and Conclusions

This paper presents a summary of structural assessment carried out at the SJH at July 2016 [3]. This evaluation began with a visual inspection survey that revealed that the current exposed condition of Column C1, was the main structural anomaly. Geometrical surveying and NDT performed during the experimental campaign (indirect and impact echo sonic testing as well as ambient vibration monitoring for OMA) assisted with developing a preliminary FEM and assigning material properties to the model. In particular, OMA results were used to calibrate the boundary conditions and the E of the masonry elements. Simulations conducted with the FEM allowed for the evaluation of the current level of stresses in the main structural elements of the SJH. Even though, numerical simulations predict that the current stress magnitudes in walls and columns are lower than their estimated compressive strengths, retrofit should be considered to stabilize the foundation of Column C1.

References

1. Palestinian Central Bureau of Statistics and the Ministry of Tourism and Antiquities (2017) Sustainable tourism - a tool for development, West Bank
2. Bacci M, Bianchi G, Campana S, Fichera G (2012) Historical and archaeological analysis of the Church of the Nativity. J Cult Heritage 13(4):e5–e26
3. Pando M, Whelan M, Ramos L, Aguilar R, Fratta D (2017) Preliminary structural and foundation assessment of the historic crusader walls and pillars at the St. Jerome Hall, Church of the Nativity, Bethlehem, University of North Carolina at Charlotte. Unpublished
4. Agisoft (2015) Agisoft PhotoScan user's Manual, release 1.2.2, Russia
5. Vasconcelos G, Lourenço PB, Alves C, Pamplona J (2008) Ultrasonic evaluation of the physical and mechanical properties of granites. Ultrasonics 48(5):453–466
6. Vasconcelos G (2005) Experimental investigations on the mechanics of stone masonry: Characterization of granites and behavior of ancient masonry shear walls
7. Miranda LF, Rio J, Guedes JM, Costa A (2012) sonic impact method–a new technique for characterization of stone masonry walls. Constr Build Mater 36:27–35
8. Van Overschee P, De Moor B (1996) Subspace identification for linear systems: theory – implementation – applications. Springer
9. TNO DIANA (2016) DIANA user's manual, release 9.6, Netherlands
10. Fotsch D, Ewins DJ (2000) Application of MAC in the frequency domain. Rolls Royce PLC-Report-PNR

11. Douglas B, Reid W (1982) Dynamic tests and system identification of bridges. J Struct Div 108(ST10)
12. Lourenço PB, Trujillo A, Mendes N, Ramos LF (2012) Seismic performance of the St. George of the Latins church: lessons learned from studying masonry ruins. Eng struct 40:501–518
13. Pluijm R (1999) Out of plane bending of masonry behaviour (Doctoral dissertation, PhD Thesis, Eindhoven University of Technology, The Netherlands)
14. Lourenço PB, Mendes N, Ramos N, Oliveira D (2011) Analysis of masonry structures without box behavior. Int J Architectural Heritage 5(4–5):369–382
15. Palchik V, Hatzor YH (2000) Correlation between mechanical strength and microstructural parameters of dolomites and limestones in the Judea group Israel. Isr J Earth Sci 49(2):65–79